Mechanics Research Communications 42 (2012) 68–76

Contents lists available at SciVerse ScienceDirect

Mechanics Research Communications

journal homepage: www.elsevier.com/locate/mechrescom

Papillary networks in the dermal–epidermal junction of skin: A biomechanical model

Pasquale Ciarletta[a], Martine Ben Amar[b,*]

[a] CNRS and Institut Jean le Rond d'Alembert, UMR7190, Place Jussieu 4, Case 162, 75005 Paris, France
[b] Laboratoire de Physique Statistique, Ecole Normale Supérieure, UPMC Univ Paris 06, Université Paris Diderot, UMR CNRS 8550, 24 rue Lhomond, 75005 Paris, France

ARTICLE INFO

Article history:
Received 27 July 2011
Received in revised form
30 November 2011
Available online 14 December 2011

Keywords:
Volumetric growth
Elastic stability
Anisotropy
Elastic bilayers
Skin

ABSTRACT

Complex networks of finger-like protrusions characterize the dermal–epidermal junction of human skin. Although formed during the foetal development, such *dermal papillae* evolve in adulthood, often in response to a pathological condition. The aim of this work is to investigate the emergence of biaxial papillary networks in skin from a mechanical perspective. For this purpose, we define a biomechanical model taking into account the volumetric growth and the microstructural properties of the dermis and the epidermis. A scalar stream function is introduced to generate incompressible transformations, and used to define a variational formulation of the boundary value elastic problem. We demonstrate that incompatible growth of the layers can induce a bifurcation of the elastic stability driving the formation of dermal papillae. Such an interfacial instability is found to depend both on the geometrical constraints and on the mechanical properties of the skin components. The results provide a mechanical interpretation of skin morphogenesis, with possible applications for micropattern fabrication in soft layered materials.

1. Introduction

The dermal–epidermal junction in human skin is characterized by the presence of complex networks of *dermal papillae*, which are finger-like structures of the dermis projecting upwards into the epidermis, as depicted in Fig. 1. Such protrusions increase the surface contact between the layers, favouring the exchange of oxygen and nutrient/waste products. The spatial distribution of the dermal papillae is detectable by staining techniques on the basement membrane of the skin (the *basal lamina*), which is a band-link sheet about 0.5–1 μm thick anchoring down the basal cells of the epidermis to the loose connective tissue of the dermis (Chan, 1997). The formation of dermal ridges starts approximately 10 weeks post-fertilization of the embryo, when small amplitude undulations of the basal laminae appear as a consequence of localized cellular proliferations in the basal layer of the epidermis (Okajima, 1975). In the following 5–7 weeks, primary ridges mature and extend deeper into the dermis forming sweat glands, whilst providing nutrients to the stem cells of the suprabasal epidermal layer, which form new skin tissue. After this period, no new dermal ridges are formed but a downfolding process occurs at the top of each primary ridge, creating a network of secondary ridges and defining the final shape of a dermal papilla, having an inter-ridge distance of about 100–200 μm and a width in the range 70–150 μm (Babler, 1991). Although human dermal ridges form first during early foetal development, they keep evolving even into adulthood, often in response to a pathological condition. For example, psoryatic abnormal proliferation results in a self-organized remodelling process characterized by an ordered (quasi-hexagonal) papillary architecture (Iizuka et al., 1999), whilst clusters of melanoma cells are often observed inside dermal papillae, creating disarrangement of the dermal–epidermal architecture before invading the dermis (Pellacani et al., 2005). Classical mathematical models have been focused on the embryonic formation of skin patterns, coupling reaction–diffusion of morphogens with chemically driven tissue interactions (Murray and Cruywagen, 1994). More recently, the role of mechanics was investigated for studying skin wrinkles (Efimenko et al., 2005) and pattern formation in fingerprints (Kucken and Newell, 2005), demonstrating that a buckling instability at the basal layer of the epidermis could explain the primary ridges. Moreover, Basan et al. (2011) have shown that dermal papillae can result from a fingering instability at the interface between a viscous fluid with a proliferation term and a viscoelastic material.

The aim of our work is to study the emergence of papillary networks from a biomechanical perspective, investigating if a differential growth between the layers can provoke a bifurcation of the elastic stability. Taking into account the microstructural properties of the

* Corresponding author.
E-mail address: benamar@lps.ens.fr (M. Ben Amar).

0093-6413/$ – see front matter © 2011 Elsevier Ltd. All rights reserved.
doi:10.1016/j.mechrescom.2011.12.001

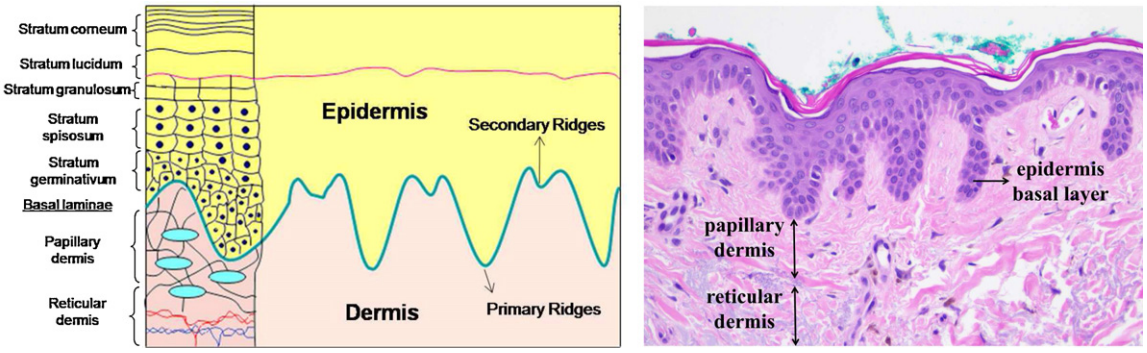

Fig. 1. Scheme of the stratified microstructure of the skin layers (left) and histological skin section showing the undulated structure of the dermal papillae (right, courtesy of Dr. P. Guitera).

dermis and the epidermis, we want to understand if the emergence of such finger-like structures can arise from a mechanical instability, as experimentally observed for the growth of soft solids under geometrical constraints (Dervaux and Ben Amar, in press). This article is organized as follows. In Section 2, we will define the biomechanical model with volumetric growth, together with an implicit kinematic description for deriving a variational formulation of the elastic problem. In Section 3, we will perform a linear stability analysis for constrained growth problems of one-layered and bi-layered models of skin tissue. The analytical solutions will be derived, and the results will be discussed in Section 4.

2. Definition of the biomechanical theory

In the following we define a biomechanical model of skin, which is considered as a hyperelastic soft tissue made of two growing layers: the dermis and the epidermis.

2.1. Kinematics and hyperelastic constitutive model

Let us consider each skin layer as a soft material having a thickness H in the direction of the z axis and lateral widths L_x, $L_y \gg H$. The elastic and the geometrical properties of adult human skin varies amongst anatomical location, sex and age of individuals. The thickness of the epidermis varies from 0.1 (eyelids) to 1.5 mm (palms and soles), whilst for the dermis it is in the range 0.3 (eyelids)–3 mm (back). Indicating with Ω_0 the fixed reference configuration of the unloaded state, the description of the deformation can be defined by a mapping χ: $\Omega_0 \to \Re^3$ that transforms the material point $\mathbf{X}\in\Omega_0$ to a position $\mathbf{x}=\chi(\mathbf{X})$ in the deformed configuration Ω. Even if surface growth models can be successfully applied to describe stretch-induced remodelling of thin skin (Buganza Tepole et al., 2011), volumetric growth should be taken into account for investigating the emergence of three-dimensional patterns. Given the deformation tensor $\mathbf{F}=\partial\chi(\mathbf{X})/\partial\mathbf{X}$, volumetric growth processes can be represented by the classical multiplicative decomposition (Rodriguez et al., 1994):

$$\mathbf{F} = \mathbf{F}_e\mathbf{F}_g \tag{1}$$

where $J=\det\mathbf{F}_g>0$ determines the volume change (in the case of isotropic homogeneous growth $\mathbf{F}_g=g\mathbf{I}$ and $J=g^3$), and $\mathbf{F}_e$ represents the elastic deformation tensor. Considering that skin tissues are basically composed of water, an incompressibility constraint must be generally imposed, so that $\det\mathbf{F}_e=1$. The epidermis is only composed of cellular matter and behaves as an isotropic material, hereafter modelled as a neo-Hookean material, so that:

$$\psi_{iso}(\mathbf{C}_e) = c_1\cdot(\mathbf{C}_e:\mathbf{I}-3) \tag{2}$$

where c_1 indicates the shear modulus and $\mathbf{C}_e$ is the elastic right Cauchy–Green strain tensor. The dermis layer is instead characterized by a strong anisotropic behaviour, due to the presence of an oriented distribution of collagen and elastin fibres, which are immersed in the ground extracellular matrix. Therefore, a general form of the strain energy density Ψ can be assumed as the sum of an isotropic and a anisotropic term (Holzapfel and Ogden, 2010), as follows:

$$\Psi = J\cdot[\psi_{iso}(\mathbf{C}_e)+\psi_{aniso}(\mathbf{C}_e,\mathbf{A}_x,\mathbf{A}_y)]-p\cdot(\det\mathbf{C}_e-1) \tag{3}$$

where p is the classical Lagrange multiplier ensuring incompressibility of the tissue, and $\mathbf{A}_x$, $\mathbf{A}_y$ are structural tensors along the principal directions of fibre reinforcements. The meshwork of the collagen and elastin fibres inside the dermis shows a preferential extensibility direction along the cleavage lines (Langer, 1978), so that a general orthotropic material behaviour can be assumed. Taking the unit vectors $\mathbf{e}_x$, $\mathbf{e}_y$ along such orthogonal directions, *the anisotropic strain energy contribution ψ_{aniso} only holds for the dermis*, and can be expressed as follows (Ciarletta et al., 2011):

$$\psi_{aniso}(\mathbf{C}_e,\mathbf{A}_x,\mathbf{A}_y) = \sum_{j=x,y}\frac{k_j}{4}\cdot(\mathbf{C}_e+\mathbf{C}_e^{-1}-2\mathbf{I}):(\mathbf{e}_j\otimes\mathbf{e}_j) \tag{4}$$

where k_x, k_y are the anisotropic material parameters determining the fibre reinforcements along the directions $\mathbf{e}_x$ and $\mathbf{e}_y$, respectively. The strain energy function defined in Eq. (4) accounts for an anisotropic stiffening both for fibre extension and compression. The positivity of the material parameters ensures polyconvexity and coerciveness of the constitutive model, other than physical consistency at large strains.

A wide variability of experimental techniques aimed at determining the stiffness of the two layers, giving a tangent elastic modulus of about 0.4–13 MPa for the dermis and 0.49–1.51 MPa for the epidermis (Agache et al., 1980; Crichton et al., 2011). In the following we will

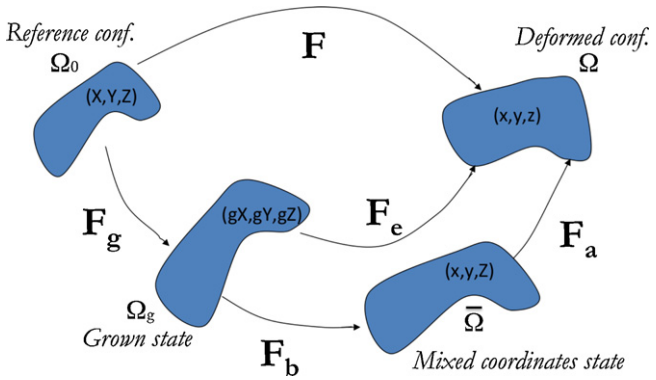

Fig. 2. Scheme of the multiplicative decomposition $\mathbf{F}=\mathbf{F}_e\mathbf{F}_g$ for volumetric growth. Considering an intermediate mixed coordinate state (x,y,Z), we can additionally set $\mathbf{F}_e=\mathbf{F}_a\mathbf{F}_b$, *with* $\mathbf{F}_a$ *and* $\mathbf{F}_b$ *given by Eqs. (5) and (6).*

propose a variational formulation of the elastic problem, based on the definition of a non-linear stream function for generating isochoric deformations.

2.2. Canonical transformation using a non-linear stream function

In the case of planar deformations, the use of a nonlinear stream function for imposing incompressibility of the elastic deformation tensor $\mathbf{F}_e$ allows a straightforward linear stability analysis for constrained growth problems (Ciarletta and Ben Amar, in press). With the aim to study the formation of complex three-dimensional instability patterns, we extend our previously developed formalism in order to transform a generic hyperelastic boundary value problem into a variational formulation. For this purpose, we use the general solution given by Ciarletta (2011) for defining isochoric transformations in the Euclidean space. In particular, we define a scalar generating function $f(x, y, Z)$ in an intermediate mixed coordinate state, so that the unknown material coordinates can be expressed in the following gradient form:

$$X=\frac{\partial^2 f(x,y,Z)}{\partial y\partial Z};\qquad Y=\frac{\partial^2 f(x,y,Z)}{\partial x\partial Z} \tag{5}$$

As shown in Fig. 2, a multiplicative decomposition $\mathbf{F}_e=\mathbf{F}_a\mathbf{F}_b$ applies to the elastic deformation tensor, which in components reads:

$$\mathbf{F}_b^{-1}=\begin{bmatrix} g\cdot f_{,xyZ} & g\cdot f_{,yyZ} & g\cdot f_{,yZZ}\\ g\cdot f_{,xxZ} & g\cdot f_{,xyZ} & g\cdot f_{,xZZ}\\ 0 & 0 & g\end{bmatrix};\quad \mathbf{F}_a=\begin{bmatrix}1 & 0 & 0\\ 0 & 1 & 0\\ z_{,x} & z_{,y} & z_{,Z}\end{bmatrix} \tag{6}$$

where $z=z(x,y,Z)$, comma denotes partial differentiation, and the growth rate g is referred to each specific layer ($g=1$ in absence of growth). Imposing the incompressibility condition $\det\mathbf{F}_e=1$ in Eq. (6), we derive an integral solution for z in the following form:

$$z=g^3\int^Z (f^2_{,xy\eta}(x,y,\eta)-f_{,xx\eta}(x,y,\eta)\cdot f_{,yy\eta}(x,y,\eta))d\eta+\beta(x,y) \tag{7}$$

where $\beta(x,y)$ is a scalar function of the two spatial coordinates, which is generally fixed by boundary conditions. Assuming that $z_{,Z}\neq 0, \pm\infty$ for avoiding local singularities in the elastic solution, Eqs. (5) and (7) give an integro-differential representation of an isochoric transformation as a function of the nonlinear stream function $f(x,y,Z)$. In the following, we will apply this kinematic formulation to derive a variational formulation of our biomechanical problem.

2.3. Variational formulation and Euler–Lagrange equations

Let us consider an isochoric transformation having the following form of the scalar generating function:

$$\mathrm{f}(x,y,Z)=xyZ+\epsilon\cdot\phi(x,y,Z) \tag{8}$$

where ϵ is a constant parameter. If $|\epsilon|\ll 1$, the scalar function $\phi(x,y,Z)$ represents the linear perturbation of the basic elastic solution. In fact, substituting Eq. (8) in Eqs. (5) and (7), the following relations hold:

$$\begin{cases} X=x+\epsilon\cdot\phi_{,yZ}; & Y=y+\epsilon\cdot\phi_{,xZ}\\ z=g^3[Z+2\epsilon\cdot\phi_{,xy}+\epsilon^2\cdot\displaystyle\int^Z(\phi^2_{,xy\eta}-\phi_{,xx\eta}\cdot\phi_{,yy\eta})d\eta] \end{cases} \tag{9}$$

In order to define a variational formulation of our biomechanical problem, let us write the total bulk potential energy Π of the continuum in the mixed coordinates, reading:

$$\Pi(x,y,Z)=\int_{\bar{\Omega}_j}\bar{\Pi}dxdydZ=\int_{x=-L_x/2}^{L_x/2}\int_{y=-L_y/2}^{L_y/2}\int_{Z=0}^{H}[\Psi(\mathbf{F}_e(\phi),\mathbf{e}_x,\mathbf{e}_y)\cdot det(\mathbf{F}_a)]dxdydZ \tag{10}$$

With the aim to take into account the elasticity of the basal lamina, we can also define a surface energy density A at the boundary $Z=H$, which reads:

$$A(x,y)=\int_{\bar{S}_j}\bar{A}\;d\bar{S}_j=\gamma\int_{x=-L_x/2}^{L_x/2}\int_{y=-L_y/2}^{L_y/2}\sqrt{1+(z_{,x})^2+(z_{,y})^2}\;dxdy \tag{11}$$

where γ represents the surface tension of the elastic membrane. Atomic force microscopy measurements of animal samples give data in the range $\gamma=0.12$–1.32 N/μm (Candiello et al., 2007). Neglecting the presence of body forces and of surface traction on the body, the linear stability problem can be defined in a variational formulation, as follows:

$$\delta\Pi(x,y,Z)+\delta A(x,y)=0 \tag{12}$$

which represents the minimization of the total elastic energy of the material. Substituting the strain energy function defined in Eqs. (2)–(4), and expanding the potential energy up to the second order in ϵ, Eq. (10) reads:

$$\begin{aligned}
&\overline{\Pi}=\frac{g(g^2-1)^2}{4}((8+4g^2)c_1+k_x+k_y)+\epsilon g^3(g^2-1)(6c_1(g^2-1)k_x+k_y))\phi_{,xyZ}\\
&+\frac{\epsilon^2}{4g}\cdot\Big\{(4g^2c_1+k_x)\phi_{,yZZ}^2+(4g^2c_1+k_y)\phi_{,xZZ}^2+g^2(4c_1+k_y+g^4k_x)\phi_{,yyZ}^2\\
&+g^2(4c_1+k_x+g^4k_y)\phi_{,xxZ}^2+2g^4(c_1(-6+30g^4)+(k_x+k_y)(3g^2-1))\phi_{,xyZ}^2\\
&+4g^8(4c_1+k_y)\phi_{,xyy}^2+4g^8(4c_1+k_x)\phi_{,xxy}^2-4g^6(4g^2c_1+u_x)\phi_{,xxy}\phi_{,yZZ}\\
&-4g^6(4g^2c_1+u_y)\phi_{,yyx}\phi_{,xZZ}+g^2(c_1(8+12g^2(1-g^4))+(k_x+k_y)(1-g^4+2g^6))\phi_{,yyZ}\phi_{,xxZ}\Big\}
\end{aligned} \tag{13}$$

Disregarding the integral term, the surface energy density can be simplified as follows:

$$\bar{A}=\gamma(1+2g^6\epsilon^2\cdot(\phi_{,xxy}^2+\phi_{,xyy}^2)) \tag{14}$$

Considering arbitrary variations of the nonlinear stream function ϕ, the volumetric Euler–Lagrange equation reads:

$$\begin{aligned}
&\left(\frac{\partial\overline{\Pi}}{\partial\phi_{,xyZ}}\right)_{,xyZ}+\left(\frac{\partial\overline{\Pi}}{\partial\phi_{,xxZ}}\right)_{,xxZ}+\left(\frac{\partial\overline{\Pi}}{\partial\phi_{,yyZ}}\right)_{,yyZ}+\left(\frac{\partial\overline{\Pi}}{\partial\phi_{,xZZ}}\right)_{,xZZ}\\
&+\left(\frac{\partial\overline{\Pi}}{\partial\phi_{,yZZ}}\right)_{,yZZ}+\left(\frac{\partial\overline{\Pi}}{\partial\phi_{,xyy}}\right)_{,xyy}+\left(\frac{\partial\overline{\Pi}}{\partial\phi_{,xxy}}\right)_{,xxy}=0
\end{aligned} \tag{15}$$

As far as the boundary conditions are concerned, the geometrical compatibility of the perturbation at a fixed surface imposes the following conditions:

$$\phi_{,xZ}=\phi_{,yZ}=\phi_{,xy}=0 \tag{16}$$

At a free surface, the Euler–Lagrange equations are derived from surface terms in the energy integrals, and read:

$$\left(\frac{\partial\overline{\Pi}}{\partial\phi_{,yZZ}}\right)_{,y}+\left(\frac{\partial\overline{\Pi}}{\partial\phi_{,xZZ}}\right)_{,x}=0 \tag{17}$$

$$\begin{aligned}
&\left(\frac{\partial\overline{\Pi}}{\partial\phi_{,xyZ}}\right)_{,xy}+\left(\frac{\partial\overline{\Pi}}{\partial\phi_{,xxZ}}\right)_{,xx}+\left(\frac{\partial\overline{\Pi}}{\partial\phi_{,yyZ}}\right)_{,yy}+\left(\frac{\partial\overline{\Pi}}{\partial\phi_{,xZZ}}\right)_{,xZ}\\
&+\left(\frac{\partial\overline{\Pi}}{\partial\phi_{,yZZ}}\right)_{,yZ}-\left(\frac{\partial\bar{A}}{\partial\phi_{,xyy}}\right)_{,xyy}-\left(\frac{\partial\bar{A}}{\partial\phi_{,xxy}}\right)_{,xxy}=0
\end{aligned} \tag{18}$$

which are obtained setting arbitrary variations $\delta\phi_{,Z}$ and $\delta\phi$, respectively. The conditions in Eqs. (17) and (18) correspond to a zero incremental stress at the free surface. In the following we use the proposed variational formalism to investigate if differential growth in skin layers can induce a bifurcation in the elastic stability localized at the dermal–epidermal junction.

3. Results

In this section we investigate the emergence of papillary structures in the dermal–epidermal junction of the skin in few constrained growth problems.

3.1. Surface instability during the constrained growth of the dermis layer

Let us first consider the case of a growing dermis layer attached at a fixed surface at $Z=0$ and free of external traction at the upper surface at $Z=H_d$. In order to study the occurrence of a biaxial surface wrinkling, mimicking the network of papillary ridges at the basal lamina, we assume the following expression for the nonlinear stream function:

$$\phi(x,y,Z)=h(Z)\sin(\kappa_x x)\sin(\kappa_y y) \tag{19}$$

representing a Z-dependent sinusoidal perturbation of the (x, y)-planes, having modes $\kappa_x = 2\pi n/L_x$, $\kappa_y = 2\pi m/L_y$, where n, m are integer numbers for satisfying the no-sliding conditions at the side surfaces. Substituting Eqs. (13) and (19) in the volumetric Euler–Lagrange equation, given by Eq. (15), the governing condition for the elastic equilibrium reads:

$$\begin{aligned}&(4g^2c_1(\kappa_x^2+\kappa_y^2)+k_y\kappa_x^2+k_x\kappa_y^2)h''''(Z)+g^2\left[\kappa_y^2(4c_1+g^4k_x+k_y)\right.\\&\left.+\kappa_x^2(4c_1+g^4k_y+k_x)+\kappa_y^2\kappa_x^2(8c_1(1+2g^6)+(g^4+1)(k_x+k_y))\right]h''(Z)\\&+4g^8\kappa_x^2\kappa_y^2(\kappa_x^2(4c_1+k_x)+\kappa_y^2(4c_1+k_y))h(Z)=0\end{aligned} \tag{20}$$

where prime denotes differentiation, and g represents the dermis growth rate. The perturbation must vanish at the fixed surface, and, from Eq. (9), the two boundary conditions read:

$$h(0)=h'(0)=0 \tag{21}$$

At the free surface $Z=H_d$, the two Euler–Lagrange equations can be simplified from Eqs. (17) and (18) as follows:

$$2g^6\kappa_y^2\kappa_x^2(8g^6c_1+K_y+K_x)h(H_d)+(4g^2c_1(\kappa_y^2+\kappa_x^2)+\kappa_y^2K_x+\kappa_x^2K_y)h''(H_d)=0 \tag{22}$$

$$\begin{aligned}&4g^6(\kappa_y^2+\kappa_x^2)\kappa_y^2\kappa_x^2\gamma h(H_d)=(4g^2c_1(\kappa_y^2+\kappa_x^2)+\kappa_y^2K_x+\kappa_x^2K_y)h'''(H_d)\\&-\kappa_x^2\kappa_y^2(8c_1(1+4g^6)+(k_x+k_y)(1+3g^4))h'(H_d)\end{aligned} \tag{23}$$

For the sake of simplicity, let us provide an analytical solution to the elastic problem setting $k_x = k_y = K$ in Eq. (4) and looking for biaxial wrinkling with $\kappa_x = \kappa_y = \kappa$. Under these assumptions, the volumetric Euler–Lagrange equation reads:

$$\left(\frac{\partial^2}{\partial Z^2}-2\kappa^2g^6\right)\left[(4c_1g^2+K)\left(\frac{\partial^2}{\partial Z^2}-2\kappa^2g^2\frac{4c_1+K}{4c_1g^2+K}\right)\right]h(Z)=0 \tag{24}$$

Taking into account the boundary condition at the fixed surface, the general solution has the following form:

$$h(Z)=h_0\left[\mathrm{Sinh}(\sqrt{2}\kappa E_gZ)-\frac{E_g}{g^3}\mathrm{Sinh}(\sqrt{2}\kappa g^3Z)+\beta(\mathrm{Cosh}(\sqrt{2}\kappa E_gZ)-\mathrm{Cosh}(\sqrt{2}\kappa g^3Z))\right] \tag{25}$$

where we have set $E_g=(\sqrt{4c_1+K}/\sqrt{4c_1+K/g^2})$. Substituting into the Euler–Lagrange condition in Eq. (17), corresponding to a vanishing incremental shear stress, we obtain the following relation:

$$\beta=\frac{(4c_1(1+g^6)+K(1+g^4))\mathrm{Sinh}(\sqrt{2}\kappa E_gH_d)-2g^3\sqrt{4c_1+K}\sqrt{4c_1+K/g^2}\mathrm{Sinh}(\sqrt{2}\kappa g^3H_d)}{2g^4(4c_1g^2+K)\mathrm{Cosh}(\sqrt{2}\kappa g^3H_d)-(4c_1(1+g^6)+K(1+g^4))\mathrm{Cosh}(\sqrt{2}\kappa E_gH_d)} \tag{26}$$

Finally, the dispersion relation of the wrinkling instability is given by the other boundary condition at the free surface, given in Eq. (18), and reads:

$$\begin{aligned}&\mathrm{A}+\mathrm{B}\cdot\mathrm{Sinh}(\sqrt{2}\kappa E_gH_d)\mathrm{Sinh}(\sqrt{2}\kappa g^3H_d)-C\cdot\mathrm{Cosh}(\sqrt{2}\kappa E_gH_d)\mathrm{Cosh}(\sqrt{2}\kappa g^3H_d)+\\&\gamma\sqrt{2}\kappa D\left[-\sqrt{4c_1+K}\mathrm{Sinh}(\sqrt{2}\kappa E_gH_d)\mathrm{Cosh}(\sqrt{2}\kappa g^3H_d)\right.\\&\left.+g^2\sqrt{4g^2c_1+K}\mathrm{Cosh}(\sqrt{2}\kappa E_gH_d)\mathrm{Sinh}(\sqrt{2}\kappa g^3H_d)\right]=0\end{aligned} \tag{27}$$

where:

$$\begin{cases}A=-4g^5(4c_1+K)(4c_1g^2+K)^{3/2}(4c_1(1+g^6)+K(1+g^4))\\B=g^3\sqrt{4c_1+K}(4c_1g^2+K)(g^8(4c_1g^2+K)^2+(4c_1(1+6g^6)+K(1+6g^4))(4c_1+K))\\C=g(4c_1+K)\sqrt{4c_1g^2+K}(4g^8(4c_1g^2+K)^2+(4c_1(1+g^6)+K(1+g^4))^2)\\D=2g^2(g^2-1)(4c_1(1+g^2+g^4)+K(1+g^2))\sqrt{4c_1g^2+K}\sqrt{4c_1+K}\end{cases} \tag{28}$$

If we neglect the presence of the surface tension, the dispersion equation reveals a threshold value $g=g^{th}$ for $\kappa\to\infty$ when $B=C$, which corresponds to a classical surface instability. In particular, this threshold value varies with the stiffness ratio K/c_1 between two asymptotic limits, $g_{iso}^{th}\le g^{th}\le g_{aniso}^{th}$,that can be calculated analytically, as follows:

$$\begin{cases}g_{aniso}^{th}=\dfrac{1}{3}(1+(19-3\sqrt{33})^{1/3}+(19+3\sqrt{33})^{1/3})\simeq 1.8392 & \text{for}\quad K/c_1\to\infty\\ g_{iso}^{th}=(g_{aniso}^{th})^{2/3}\simeq 1.5011 & \text{for}\quad K/c_1=0\end{cases} \tag{29}$$

As discussed in Ben Amar and Ciarletta (2010), the presence of a capillary energy can fix the wavelength at threshold because it introduces a typical length-scale d_{cap} in the system, which is given by $d_{iso}=\gamma/c_1$ or $d_{aniso}=\gamma/K$. From the dispersion relation in Eq. (27), we derive that capillarity induces a small correction to the analytical threshold g^{th}, such that the new threshold value is given by $g^*=g^{th}+\eta d_{cap}$, where η can be found by series expansion of Eq. (27) around g^{th}. In particular, the wavenumber at threshold can be found as follows:

$$\sqrt{2}\kappa^{th}=\frac{1}{2E_gH_d}\mathrm{Log}\left[\frac{B+C}{C-B}\right] \tag{30}$$

which in series expansion over $(g^* - g^{th})$ gives the following asymptotic limits:

$$\begin{cases} \sqrt{2}\kappa^{th}_{aniso} = \dfrac{1}{2H_d g^{th}_{aniso}} \mathrm{Log}\left[\dfrac{4.985}{g^* - g^{th}_{aniso}}\right] & \text{for} \quad K/c_1 \to \infty \\ \sqrt{2}\kappa^{th}_{iso} = \dfrac{1}{2H_d} \mathrm{Log}\left[\dfrac{2.7126}{g^* - g^{th}_{iso}}\right] & \text{for} \quad K/c_1 = 0 \end{cases} \tag{31}$$

Moreover, we find the typical logarithmic correction of the threshold and the wavelength λ^{th} at first order in $(g^* - g^{th})$, which in the general case read:

$$\lambda^{th} = (4\sqrt{2}\pi H_d)/\mathrm{Log}\left[\frac{\tau H_d}{d_{cap}}\right]; \qquad g^* = g^{th} + \eta \frac{d_{cap}}{H_d} \mathrm{Log}\left[\frac{\tau H_d}{d_{cap}}\right] \tag{32}$$

where η, τ are constants depending on the stiffness ratio K/c_1. Summarizing, we obtain that a critical volume increase in the dermal layer determines the occurrence of a surface instability, depending on the ratio between isotropic and anisotropic elastic moduli. Moreover, the surface energy of the basal lamina fixes the wavelength of such an instability, providing a logarithmic correction to the growth threshold value.

3.2. Papillary ridges formed by an epidermal layer growing on a nonlinear elastic dermis

Let us now consider the case where a growing epidermal layer is attached at its bottom to the dermis, whose thickness and elastic modulus are indicated with H_e, H_d and c_{1e}, c_{1d} in the following. In this example, we consider that only the epidermis undergoes a volumetric growth process, and we set the reference plane $Z = 0$ at the fixed dermal surface. The solution of the governing equilibrium equation for the dermis, given by Eq. (24) in absence of growth, reads as follows:

$$h_d(Z) = f_d[(Z - d_d)\mathrm{Sinh}(\sqrt{2}\kappa Z) - \sqrt{2} d_d \kappa Z \cdot \mathrm{Exp}[-\sqrt{2}\kappa Z]] \tag{33}$$

where f_d, d_d are constant parameters, and it is assumed that its bottom surface is fixed to a rigid substrate, i.e. $h_d(0) = h'_d(0) = 0$. In practice, we aim at representing the situation where $H_d < H_e$, so that the growth instability is localized in a boundary layer at the dermal–epidermal junction. Under these assumptions, the solution of the perturbed solution for the epidermal layer can be simplified as follows:

$$h_e(Z) = \alpha_d[\mathrm{Exp}[-\sqrt{2}\kappa Z] + \beta_d \cdot \mathrm{Exp}[-\sqrt{2} g^3 \kappa Z]] \tag{34}$$

which automatically vanishes for $Z \gg H_d$, with g representing the growth rate of the epidermis. Therefore, in order to solve this bi-layered growth model of skin, we need to impose four boundary conditions at $Z = H_d$. The first two are given by imposing the continuity of the displacement fields at the interface, and read:

$$g^3 h_e(H_d) - h_d(H_d) = 0; \qquad h'_e(H_d) = h'_d(H_d) \tag{35}$$

The vanishing conditions of the surface terms in Eqs. (17) and (18) correspond to the continuity of the shear and normal stresses across the interface, and give the remaining two Euler–Lagrange boundary equations:

$$(4c_{1d} + K_d)(2\kappa^2 h_d(H_d) + h''_d(H_d)) = (4g^2 c_{1e})(2\kappa^2 g^6 h_e(H_d) + h''_e(H_d)) \tag{36}$$

$$\begin{aligned} &6\kappa^2(4c_{1d} + K_d)h'_d(H_d) - (4c_{1d} + K_d)h'''_d(H_d)) + 8\kappa^2 \gamma h_d(H_d) \\ &= 2\kappa^2 g^2 (4c_{1e}(1 + 2g^6))h'_e(H_d) - (4g^2 c_{1e})h'''_e(H_d) \end{aligned} \tag{37}$$

where K_d is the anisotropic elastic modulus of the dermis. Neglecting the presence of the capillary energy and of the material anisotropy in the dermis, the dispersion relation $D_d = 0$ can be obtained substituting the perturbations in Eqs. (33) and (34) into the boundary conditions in Eqs. (35)–(37), as follows:

$$D_d = \mathrm{A}_d + B_d \mathrm{Cosh}(2\sqrt{2}\kappa H_d) - C_d \mathrm{Sin}(2\sqrt{2}\kappa H_d) = 0 \tag{38}$$

with:

$$\begin{cases} A_d = 8g^2(g^6 - 1)H_d^2\kappa^2 \dfrac{c_{1d}}{c_{1e}} - (1 + 4H_d^2\kappa^2)\left(4\left(\dfrac{c_{1d}}{c_{1e}}\right)^2 + g^4(g^9 - 3g^6 - g^3 - 1)\right) \\ B_d = -4\left(\dfrac{c_{1d}}{c_{1e}}\right)^2 + g^4(g^9 - 3g^6 - g^3 - 1) \\ C_d = 4\left(\dfrac{c_{1d}}{c_{1e}}\right) g^2(g^3 + 1) \end{cases} \tag{39}$$

Considering the limit $c_{1d}/c_{1e} \ll 1$, and imposing simultaneously $D_d = 0$ and $\partial D_d/\partial(\kappa H_d) = 0$ in Eq. (38), we derive that a basal laminae undulation first occurs at the growth rate threshold g^* such that $B_d = C_d$. In particular, this threshold correction at first order in c_{1d}/c_{1e} is given by:

$$g^* = g^{th}_{iso} + 0.8719 \cdot \frac{c_{1d}}{c_{1e}} \tag{40}$$

As shown in Fig. 3 (left), such an asymptotic value depends on the ratio between elastic moduli c_{1d}/c_{1e}, recovering the analytical threshold g^{th}_{iso} in Eq. (29) if c_{1d}=0. In the same way, when considering the limit $(c_{1d}/c_{1e}) \gg 1$, we can derive a threshold scaling $g^{th} \simeq (2c_{1d}/c_{1e})^{2/13}$,

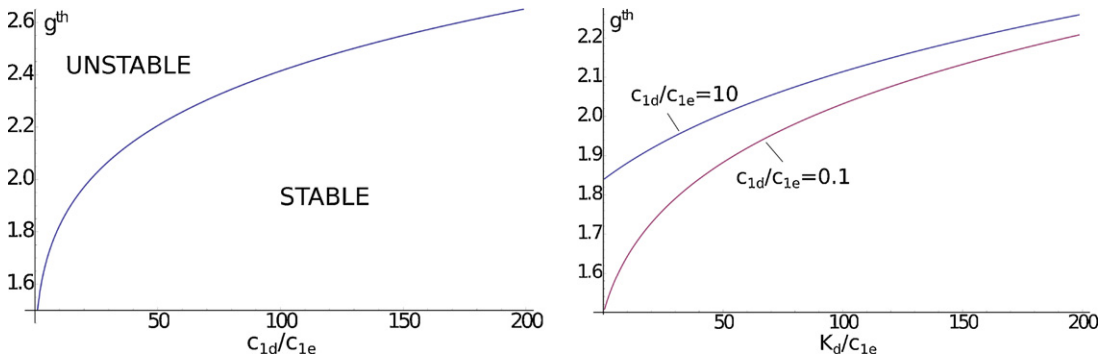

Fig. 3. Asymptotic value of the epidermal growth threshold g^{th} depicted with respect to the elastic ratio c_{1d}/c_{1e} (left, K_d=0) and to K_d/c_{1e} (right).

recovering the fact that an infinite growth is required if the epidermis tends to be rigid. If in the one-layered model of skin the growth threshold indicated a surface instability with $\kappa \to \infty$, in this bilayer model we find that the instability wavenumber is fixed to a finite value. This results is rather intuitive because the dermis elasticity introduces a typical lengthscale corresponding to $d_d = H_d c_{1d}/c_{1e}$. Considering the limit $c_{1d}/c_{1e} \ll 1$, and substituting the threshold condition $B_d = C_d$ in the dispersion relation in Eq. (38), the instability wavelength is given by solving:

$$\mathrm{Cosh}(2\sqrt{2}\kappa H_d) - \mathrm{Sinh}(2\sqrt{2}\kappa H_d) = -\left((g_{iso}^{th})^3 - 1\right) 2\kappa^2 H_d^2 + (1 + 4\kappa^2 H_d^2) \tag{41}$$

which gives the following threshold wavelength:

$$\lambda^{th} = \frac{2\pi}{\kappa^*} \simeq \frac{2\pi H_d \sqrt{2}}{1.58} = 5.62 H_d \tag{42}$$

Finally, the presence of the surface energy of the basal lamina has the same effect discussed in the previous paragraph, introducing a capillary length in the problem which provides a logarithmic correction to the growth rate threshold value. The instability pattern at threshold will result from a competition between these two lengthscales d_d and d_{cap}. However, further derivation in this sense will be neglected for matter of notation compactness.

3.3. *Papillary ridges formed by a growing dermis under a soft epidermis layer*

In this last example, let us consider a growing portion of the papillary dermis attached at $Z = 0$ to a fixed substrate and in contact at $Z = H_d$ to a thicker epidermis layer, so that $H_e \gg H_d$. In such a case, the perturbed solutions of the volumetric Euler–Lagrange equation read:

$$h_d(Z) = f_e \left\{ d_e[\mathrm{Cosh}(\sqrt{2}\kappa E_g Z) - \mathrm{Cosh}(\sqrt{2} g^3 \kappa Z)] + \mathrm{Sinh}(\sqrt{2}\kappa E_g Z) - E_g \frac{\mathrm{Sinh}(\sqrt{2} g^3 \kappa Z)}{g^3} \right\} \tag{43}$$

$$h_e(Z) = \alpha_e[\mathrm{Exp}[-\sqrt{2}\kappa Z] + \beta_e Z \cdot \mathrm{Exp}[-\sqrt{2}\kappa Z]] \tag{44}$$

where g is the isotropic growth rate of the dermis layer and $E_g = (\sqrt{4c_{1d} + K_d}/\sqrt{4c_{1d} + K_d/g^2})$. The two boundary conditions corresponding to the continuity of the perturbation fields across the interface are given by:

$$h_e(H_d) - g^3 h_d(H_d) = 0; \qquad h_e'(H_d) = h_d'(H_d) \tag{45}$$

The remaining two Euler–Lagrange equations in Eqs. (17) and (18) can be rewritten at $Z = H_d$ as follows:

$$4c_{1e}(2\kappa^2 h_e(H_d) + h_e''(H_d)) = (4g^2 c_{1d} + K_d)(2\kappa^2 g^6 h_d(H_d) + h_d''(H_d)) \tag{46}$$

$$\begin{aligned} &c_{1e}(24\kappa^2 h_e'(H_d) - 4h_e'''(H_d)) - 8\kappa^4 g^7 \gamma h_d(H_d) \\ &= 2\kappa^2 g^2 (4c_{1d}(1 + 2g^6) + K_d(1 + 2g^4)) h_d'(H_d) - (4g^2 c_{1d} + K_d) h_d'''(H_d) \end{aligned} \tag{47}$$

Substituting Eqs. (43) and (44) into the four boundary conditions given in Eqs. (45)–(47), we find the following simplified expression of the dispersion relation for the interfacial instability:

$$\begin{aligned} &A_d + \mathrm{Cosh}(g^3\sqrt{2}\kappa H_d)(B_{d1}\mathrm{Cosh}(\sqrt{2}\kappa H_d) + B_{d2}\mathrm{Sinh}(\sqrt{2}\kappa H_d)) \\ &+\mathrm{Sinh}(g^3\sqrt{2}\kappa H_d)(C_{d1}\mathrm{Cosh}(\sqrt{2}\kappa H_d) + C_{d2}\mathrm{Sinh}(\sqrt{2}\kappa H_d)) = 0 \end{aligned} \tag{48}$$

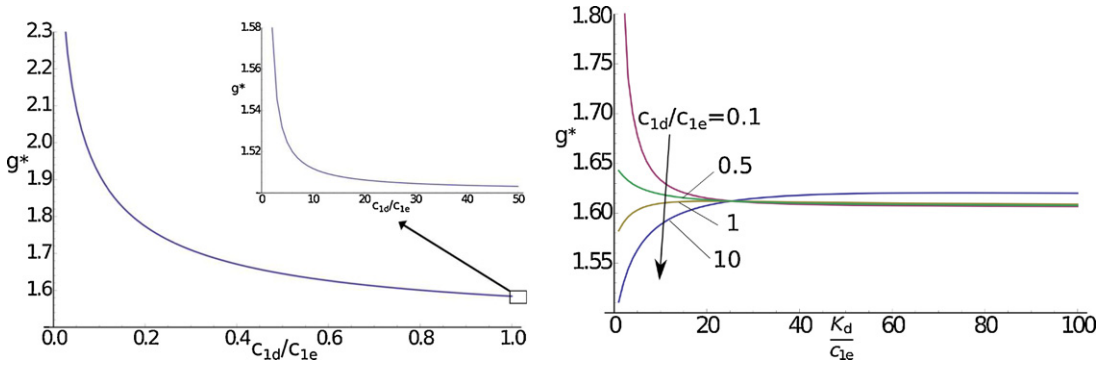

Fig. 4. Asymptotic value of the dermis growth threshold g^* depicted with respect to the elastic ratio c_{1d}/c_{1e} (left, K_d=0; inset: rescaled zone with c_{1d}/c_{1e}>1) and to K_d/c_{1e} (right).

where:

$$\begin{cases} A_d = 8\sqrt{2}g^3 - 4\sqrt{2}\left(\dfrac{c_{1d}}{c_{1e}}\right)^2 g^8(1+g^6) - 3\sqrt{2}\dfrac{c_{1d}}{c_{1e}}(g^2-1)(1+3g^6) + 4g^5\kappa d_{cap} \\ B_{d1} = -4g^3(2\sqrt{2}+g^2\kappa d_{cap}) + 3\sqrt{2}\dfrac{c_{1d}}{c_{1e}}(g^2-1)(1+3g^6) + \sqrt{2}\left(\dfrac{c_{1d}}{c_{1e}}\right)(g^2+2g^8+5g^{14}) \\ B_{d2} = \dfrac{c_{1d}}{c_{1e}}(g^6-1)(2\sqrt{2}(g^5-1)+g^7\kappa d_{cap}) \\ C_{d1} = -\dfrac{c_{1d}}{c_{1e}}g^2(g^6-1)(2\sqrt{2}(1-g)+g^2\kappa d_{cap}) \\ C_{d2} = 2(g^6+1)(2\sqrt{2}+g^2\kappa d_{cap}) - 3\sqrt{2}\dfrac{c_{1d}}{c_{1e}}g^3(g^2-1)(3+g^6) - \sqrt{2}\left(\dfrac{c_{1d}}{c_{1e}}\right)^2(g^5+6g^{11}+g^{17}) \end{cases} \tag{49}$$

with $d_{cap} = \gamma/c_{1e}$. Such coefficients are written in the case $K_d = 0$ for matters of notation compactness; nevertheless, the influence of K_d on the elastic stability is depicted in Fig. 4 (right). When $d_{cap}/H_d \to 0$, the isotropic dispersion relation in Eq. (48) highlights the occurrence of a surface instability with $\kappa \to \infty$ when $(B_{d1} + B_{d2} + C_{d1} + C_{d2}) = 0$. In particular, for $c_{1d} \gg c_{1e}$ the system corresponds to the monolayer case, and we derive the same growth instability threshold g^{th}_{iso}. The variability of such an instability threshold g^* with the elastic material parameters is shown in Fig. 4. If $d_{cap}/H_d \ll 1$ we can make a series expansion of Eq. (48) to quantify the effect of capillarity on the threshold values. Taking the realistic values $d_{cap}/H_d = 0.0001$ and $c_{1d}/c_{1e} = 0.3$, the corrections are given by:

$$g^{th} = g^* + 0.1445\ \frac{d_{cap}}{H_d}\cdot \mathrm{Log}\left[\frac{1.5268H_d}{d_{cap}}\right]; \qquad \lambda^{th} = (4\sqrt{2}\pi H_d)/\mathrm{Log}\left[\frac{1.5268H_d}{d_{cap}}\right] \simeq 1.84H_d \tag{50}$$

The structure of the dispersion relation is the same as the one studied for the monolayer model of dermis growth, and we find again that the basal lamina elasticity imposes a logarithmic correction of the growth rate threshold value, whilst fixing the wavelength of the perturbation.

4. Discussion and conclusion

In this work, we have studied the formation of biaxial networks of papillary structures emerging at the dermal–epidermal junction of the skin. For this purpose, we have defined a biomechanical model of volumetric growth processes of the two upper skin layers, taking into account the different structural properties of the epidermis and the dermis in Eqs. (2) and (3). In particular, the presence of collagen and elastin fibres embedded in the extracellular matrix of the dermis required the definition of a suitable anisotropic strain energy function, given in Eq. (4). Differential growth between the two layers, together with generic geometrical constraints, can induce residual strains inside these two skin layers, which may ultimately provoke a bifurcation of the elastic stability at their interface. Instead of the classical method of incremental elastic deformations (Ogden, 1997), we perform the linear stability analysis using a novel variational formulation of the boundary elastic problem. Defining a nonlinear stream function in a mixed coordinate state, we are able to generate an implicit description of isochoric transformations in Eqs. (5) and (7). The boundary value problem can be solved by minimization of the total elastic energy of the tissue, given by Eq. (12). The governing elastic equations correspond to the Euler–Lagrange equations, which are expressed in Eqs. (15), (17) and (18), and are solved in the linear stability analysis of different constrained growth problems. Considering first the isotropic growth of a surface-attached dermis, with a surface energy representing the elastic contribution of the basement membrane and of the epidermis, we find that a surface wrinkling occurs at a threshold volume change. Such a threshold value increases with increasing anisotropic stiffening, and we recover in Eq. (29) the analytical limit $g^{th}_{iso} \simeq 1.5011$ for an isotropic material, which corresponds to the compressive strain $\varepsilon_c = 1 - 1/g^{th}_{iso} \simeq 0.33$ found in the experiments of Trujillo et al. (2008) on hydrogels. Critical strain threshold for crease formation was numerically calculated by Hong et al. (2009) at $\varepsilon_{cr} = \simeq 0.35$, predicting the emergence of a local singularity in the vicinity of our linear stability threshold. Such a biaxial wrinkling results from a surface instability mechanism, first considered by Biot (1963), which is regularized at threshold by the surface energy (Ben Amar and Ciarletta, 2010). The wrinkling wavelength λ scales with the thickness H_d of the layer and is fixed by the presence of a typical lengthscale d_{cap} (i.e. the ratio between the surface energy and the dominant elastic modulus), with a general relation given in Eq. (32). A bilayered model of skin fixed at the bottom surface of the dermis is later investigated, considering separately the volumetric growth of one layer attached to the other through an elastic basement membrane. Having the aim to

study the undulation patterns localized in a boundary layer across the dermal–epidermal junction, we only focused on the elastic solutions vanishing at the free skin surface, deriving the dispersion relations in Eqs. (38) and (48). In the case of epidermal growth on a surface-attached dermis, in the limit $c_{1d}/c_{1e} \to 0$ a biaxial papillary pattern occurs at the threshold growth rate in Eq. (40), with a wavelength that scales with the dermis thickness, as expressed in Eq. (42). Therefore, the interface wrinkling of a thick film is very different from the surface folding of a thin film on a soft substrate, characterized by a wavelength scaling of the order $H_e(c_{1e}/c_{1d})^{1/3}$ (Sultan and Boudaoud, 2008). In our case, the variation of the growth threshold with the elastic moduli is depicted in Fig. 3, showing a scaling $g^{th} \propto (c_{1d}/c_{1e})^{2/13}$ where $c_{1d}/c_{1e} \gg 1$, in agreement with the results of Dervaux and Ben Amar (2011) for a thick ring of gel growing on a stiff core. When considering the dermis growth under a thick epidermis layer, we find again a surface instability occurring at a growth threshold depending on the elastic parameters (diverging for c_{1d}/c_{1e}, $K_d/c_{1e} \to 0$, see Fig. 4), whilst the short wavelength instability is fixed by the elasticity of the basement membrane. If for $c_{1d}/c_{1e} \gg 1$ we recover the asymptotic limit calculated for the monolayer case, the role of anisotropic reinforcements becomes here crucial. In the previous cases anisotropy had always a stabilizing effect, here an increasing fibre reinforcement lowers (increases) the growth threshold when $c_{1d}/c_{1e} < 1$ ($c_{1d}/c_{1e} \geq 1$). This effect is rather important when dealing with aging phenomena, suggesting that changes of mechanical parameters over time alone can provoke mechanical instabilities in a layered tissue. In conclusion, we have demonstrated that incompatible growth processes inside the skin can drive the emergence of complex biaxial networks of dermal papillae. The characteristics of such an interfacial instability strongly depend on the geometrical constraints of the problem and on the mechanical parameters of the two main layers. In particular, the presence of anisotropic fibre reinforcement in the dermis has a paramount importance for determining the growth instability threshold, whilst the elasticity of the basal membrane determines the pattern periodicity at threshold. Although the simplificative assumptions in our model allowed to derive an analytical solution, further work will be needed in order to investigate the effects of inhomogeneous growth processes in the stratified microstructure of the skin layers. Our results can help understanding growth morphologies of biological tissues in health and pathological conditions (Richman et al., 1975), as well as guiding the fabrication of specific micropatterns in thin layered materials (Wang et al., 2011).

Acknowledgements

We are thankful to Pascale Guitera, Sidney Melanoma Diagnostic Center, for providing the image in Fig. 1. P.C. has been partially funded by the Marie Curie grant ERG-256605, EC FP7 program.

References

Agache, P.G., Monneur, C., Leveque, J.L., De Rigal, J., 1980. Mechanical properties and Young's modulus of human skin in vivo. Arch. Dermatol. Res. 269, 221–232.
Babler, W.J., 1991. Embryologic development of epithelial ridges and their configurations. Birth Defects Orig. 27 (02), 95–112.
Basan, M., Joanny, J.F., Prost, J., Risler, M., 2011. Undulation instability of epithelial tissues. Phys. Rev. Lett. 106, 158101.
Ben Amar, M., Ciarletta, P., 2010. Swelling instability of surface-attached gels as a model for soft tissue growth under geometric constraints. J. Mech. Phys. Solids 58, 935–954.
Biot, M.A., 1963. Surface instability of rubber in compression. Appl. Sci. Res. A 12, 168–182.
Buganza Tepole, A., Ploch, C.J., Wong, J., Gosain, A.K., Kuhl, E., 2011. Growing skin: a computational model for skin expansion in reconstructive surgery. J. Mech. Phys. Solids 59, 2177–2190.
Chan, L.S., 1997. Human skin basement membrane in health and in autoimmune diseases. Front. Biosci. 2, d343–352.
Candiello, J., Balasubramani, M., Shreiber, E.M., Cole, G.J., Mayer, U., Halfter, W., Lin, H., 2007. Biomechanical properties of native basement membranes. FEBS J. 274, 2897–2908.
Ciarletta, P., Ben Amar, M. Growth instabilities and folding in tubular organs: a variational method in nonlinear elasticity, Int. J. Non-linear Mech., doi:10.1016/j.ijnonlinmec.2011.05.013, in press.
Ciarletta, P., Izzo, I., Micera, S., Tendick, F., 2011. Stiffening by fiber reinforcement in soft materials: a hyperelastic theory at large strains and its application. J. Biomech. Behavior Biomed. Mater. 4, 1359–1368.
Ciarletta, P., 2011. Generating functions for volume-preserving transformations. Int. J. Non-linear Mech. 46 (9), 1275–1279.
Crichton, M.L., Donose, B.C., Chen, X., Raphael, A.P., Huang, H., Kendall, M.A., 2011. The viscoelastic, hyperelastic and scale dependent behaviour of freshly excised individual skin layers. Biomaterials 32, 4670–4681.
Dervaux, J., Ben Amar, M., 2011. Buckling condensation in constrained growth. J. Mech. Phys. Solids 59, 538–560.
Dervaux, J., Ben Amar, M., 2012. Mechanical instabilities of gels. Annu. Rev. Condens. Matter Phys. 3, 9.1–9.22.
Efimenko, K., Rackaitis, M., Manias, E., Vaziri, A., Mahadevan, L., Genzer, J., 2005. Nested self-similar wrinkling patterns in skin. Nat. Mater. 4, 293–297.
Holzapfel, G.A., Ogden, R.W., 2010. Constitutive modeling of arteries. Proc. R. Soc. A: Math. Phys. 466, 1551–1597.
Hong, W., Liu, Z., Suo, Z., 2009. Formation of creases on the surfaces of elastomers and gels. Appl. Phys. Lett. 95, 111901.
Iizuka, H., Honda, H., Ishida-Yamamoto, A., 1999. Epidermal remodeling in psoriasis (III): a hexagonally-arranged cylindrical papilla model reveals the nature of psoriatic architecture. J. Dermatol. Sci. 21, 105–112.
Kucken, M., Newell, A.C., 2005. Fingerprint formation. J. Theor. Biol. 235, 71–83.
Langer, K., 1978. On the anatomy and physiology of the skin: I. the cleavability of the cutis. Br. J. Plast. Surg. 31 (1), 3–8.
Murray, J.D., Cruywagen, G.C., 1994. Threshold bifurcation in tissue interaction models for spatial pattern generation. Phil. Trans. R. Soc. Lond. A 347, 661–676.
Ogden, R.W., 1997. Non-linear Elastic Deformations. Dover, New York.
Okajima, M., 1975. Development of dermal ridges in the fetus. J. Med. Genet. 12, 243–250.
Pellacani, G., Cesinaro, A.M., Longo, C., Grana, C., Seidenari, S., 2005. Microscopic in-vivo description of cellular architecture of dermoscopic pigment network in nevi and melanomas. Arch. Dermatol. 141, 147–154.
Richman, D.P., Stewart, R.M., Hutchinson, J.W., Caviness, W.S., 1975. Mechanical model of brain convolutional development. Science 189, 18–21.
Rodriguez, E.K., Hoger, A., McCulloch, A., 1994. Stress-dependent finite growth in soft elastic tissues. J. Biomech. 27, 455–467.
Sultan, E., Boudaoud, A., 2008. The buckling of a swollen thin gel layer bound to a compliant substrate. J. Appl. Mech. 75, 051002.
Trujillo, V., Kim, J., Hayward, R.C., 2008. Creasing instability of surface-attached hydrogels. Soft Matter 4, 564–569.
Wang, Q., Zhang, L., Zhao, X., 2011. Creasing to cratering instability in polymers under ultrahigh electric fields. Phys. Rev. Lett. 106, 118301.